Independent Trajectory Implementation of the Semiclassical Liouville Method: Application to Multidimensional Reaction Dynamics†

Eduardo Roman and Craig C. Martens*

Department of Chemistry, University of California, Irvine, Irvine, California 92697-2025

Received: April 3, 2007

We describe an independent trajectory implementation of semiclassical Liouville method for simulating quantum processes using classical trajectories. In this approach, a single ensemble of trajectories describes all semiclassical density matrix elements of a coupled electronic state problem, with the ensemble evolving classically under a single reference Hamiltonian chosen on the basis of physical grounds. In this paper, we introduce an additional uncoupled trajectory approximation, allowing the members of the ensemble to evolve independently of one another and eliminating the major computational costs of our previous coupled trajectory implementation. The accuracy of the method is demonstrated for model one-dimensional problems. In addition, the approach is applied to the chemical reaction dynamics of a collinear triatomic system, yielding excellent agreement with exact calculations. This method allows molecular dynamics involving coupled electronic surfaces to be modeled with essentially the same effort as classical molecular dynamics and ensemble averaging.

I. Introduction

In this paper, we describe a method for simulating the dynamics of molecular systems with coupled electronic states based on a semiclassical limit of the coupled state Liouville equation.[1−7] Our previous work has demonstrated that accurate results can be obtained in principle for model one-dimensional systems using the semiclassical Liouville method. Here, we introduce additional approximations that allows the method to be applied to *multidimensional* problems with an effort comparable with purely classical molecular dynamics and ensemble averaging.

In the semiclassical Liouville method, the leading quantum electronic coherence effects are incorporated by extending the conventional classical description of nonadiabatic transitions in terms of trajectories to include an explicit semiclassical ensemble-based treatment of the off-diagonal electronic coherence.[1−7] Similar approaches have been pursued by Kapral, Ciccotti, and co-workers,[8−11] Schofield and co-workers,[12−14] Ando and co-workers,[15,16] Stock and co-workers,[17] and others.

In our previous publications, we describe the nonadiabatic semiclassical Liouville formalism and present numerical implementations of the general approach in the context of a modified classical molecular dynamics simulation in both diabatic[1,2,4,5] and adiabatic[3] representations. In addition, we apply the method to the simulation of quantum electronic coherence and the process of environmental decoherence.[4,6,18] The method has proven to be quite accurate for the model problems considered so far, providing not only nearly quantitative agreement between the observable electronic population transfer but also a faithful representation of the evolving states of the system, including the intrinsically quantum mechanical coherence terms.

A full numerical implementation of the semiclassical Liouville method for nonadiabatic dynamics is computationally intensive,[1−4,18] and care must be taken in the selection and propagation of the trajectory ensembles. These complications are due to the use of *multiple* ensembles, each representing an element of the semiclassical density matrix ρ_{ij}. Each trajectory ensemble evolves under its own Hamiltonian in the multiple ensemble implementation, and thus the relative positions of the trajectories must be carefully followed. Often, the ensembles diverge from each other under their intrinsic dynamics, leading to numerical problems and requiring birth, death, or retirement of the trajectories. Although our previous work demonstrated that a full implementation of the method can give quantitatively accurate results in principle, simplification of the numerical algorithm is needed to apply the approach in practice to realistic multidimensional problems.

The numerical effort can be reduced in some applications by reformulating the general semiclassical Liouville method in terms of a single trajectory ensemble.[7] Here, *one* ensemble of trajectories supports the evolution of *all* of the generalized phase space distributions $\rho_{ij}(q, p, t)$. A single reference Hamiltonian is chosen on the basis of physical grounds; for electronic relaxation of an initially excited state, the upper surface Hamiltonian H_{11} is the natural choice, for instance. Classical trajectories evolving on this surface then represent the dynamics of the population of the upper state $\rho_{11}(q, p, t)$ *and also* the electronic coherence $\rho_{12}(q, p, t)$ and ground state population $\rho_{22}(q, p, t)$. The error made in the classical motion of the trajectories for these latter distributions is compensated for by incorporating the difference between the correct and reference Liouville propagators into the calculation of the coefficients of the individual trajectories. As illustrated in ref 7, this approach can give nearly exact results for a number of model problems and cases describing ultrafast electronic relaxation dynamics. Although the single ensemble method is much simpler to implement than the full multiple ensemble approach, the interaction of trajectories within the ensemble leads to numerical challenges in multidimensional systems, where the large number of trajectories required to sample the evolving densities combined with the linear algebra problem associated with trajectory interactions leads to high computational expense.

† Part of the special issue "Robert E. Wyatt Festschrift".

* Corresponding author. E-mail: cmartens@uci.edu.

10.1021/jp072629v CCC: $37.00
Published on Web 07/18/2007

In this paper, we describe the extension of the semiclassical Liouville method to problems in multiple dimensions. We introduce an *independent trajectory approximation*, where the computationally expensive terms in the equations of motion that capture the nonlocality of nuclear quantum dynamics are neglected. The resulting method, although quantum mechanical in nature, resembles conventional classical molecular dynamics and ensemble averaging in practical implementation. As we describe below, this approximation is often (although not always) a good one, leading to an efficient and easily implemented method for modeling molecular dynamics on multiple electronic states in many dimensions.

The organization of the rest of this paper is as follows: In section II, we briefly review the semiclassical Liouville approach to molecular dynamics on multiple electronic states. We summarize the multiple ensemble methodology employed in our previous work and describe the current single ensemble−independent trajectory formulation. In section III, we apply the method to model single and multidimensional problems and compare the results with exact quantum wave packet calculations. Finally, a summary is given in section IV.

II. Method

We consider the problem of nonadiabatic molecular dynamics on two coupled electronic surfaces. The time-dependent wave function describing the coupled electronic-nuclear dynamics of a two electronic state f nuclear degree of freedom system is given by

$$\Psi(\mathbf{q}, t) = \begin{pmatrix} \psi_1(\mathbf{q}, t) \\ \psi_2(\mathbf{q}, t) \end{pmatrix} \tag{1}$$

and the Hamiltonian is a 2×2 matrix of operators:

$$\hat{H} = \begin{pmatrix} \hat{H}_{11} & V \\ V & \hat{H}_{22} \end{pmatrix} \tag{2}$$

where $\mathbf{q} = (q_1, q_2, ..., q_f)$. The diagonal elements $\hat{H}_{jj}$ consist of the kinetic plus single surface potential energy operators,

$$\hat{H}_{jj} = \sum_{n=1}^{f} \frac{\hat{p}_n^{\,2}}{2m_n} + U_j(\mathbf{q}) \tag{3}$$

for $i = 1, 2$. We take the off-diagonal element $V(\mathbf{q})$ to be a real function of the coordinates $\mathbf{q}$; this corresponds to a diabatic representation of the electronic problem.[19]

Our semiclassical approach to nonadiabatic molecular dynamics is based on the quantum Liouville equation for the density operator $\hat{\rho}(t)$.[20,21] The Liouville representation allows a direct analogy to be made between classical and quantum mechanics and permits a description of manifestly quantum mechanical quantities and processes in terms of classical functions in phase space and their approximations by trajectory ensembles.

The state of the system is described by the density operator $\hat{\rho}(t)$, which obeys the quantum Liouville equation[20,21]

$$i\hbar \frac{d\hat{\rho}(t)}{dt} = [\hat{H}, \hat{\rho}(t)] \tag{4}$$

For the two state problem considered here, the density operator is itself a 2×2 matrix,

$$\hat{\rho}(t) = \begin{pmatrix} \hat{\rho}_{11}(t) & \hat{\rho}_{12}(t) \\ \hat{\rho}_{21}(t) & \hat{\rho}_{22}(t) \end{pmatrix} \tag{5}$$

Written out explicitly in terms of components of $\hat{\rho}$, eq 4 becomes

$$i\hbar \frac{d\hat{\rho}_{ij}}{dt} = \sum_{k=1}^{2} \hat{H}_{ik}\hat{\rho}_{kj} - \hat{\rho}_{ik}\hat{H}_{kj} \tag{6}$$

where $\hat{H}_{12} = \hat{H}_{21} = V$.

The classical limit of the multistate quantum Liouville equation of motion can be found by applying the Wigner−Moyal formalism,[22−25] which gives a classical phase space representation of the algebra of quantum operators in terms of a power series expansion in $\hbar$. To lowest order, the product of two operators $\hat{A}$ and $\hat{B}$ becomes

$$\hat{A}\hat{B} = AB + i\hbar\{A, B\} + O(\hbar^2) \tag{7}$$

where $A(\mathbf{q}, \mathbf{p})$ and $B(\mathbf{q}, \mathbf{p})$ are the corresponding functions defined on phase space $(\mathbf{q}, \mathbf{p})$ and

$$\{A, B\} = \sum_n \left(\frac{\partial A}{\partial q_n} \frac{\partial B}{\partial p_n} - \frac{\partial B}{\partial q_n} \frac{\partial A}{\partial p_n} \right)$$

is the Poisson bracket.[26] A systematic power series in $\hbar$ can be defined rigorously for general operators depending on $\hat{q}_n$ and $\hat{p}_n$ using the Wigner-Moyal formalism. This classical limit results in a set of coupled partial differential equations for the semiclassical phase space functions corresponding to the matrix elements of $\hat{\rho}$. These are[1−4,18]

$$\frac{\partial \rho_{11}}{\partial t} = \hat{\mathscr{L}}_{11}\rho_{11} + \{V, \mathrm{Re}\ \rho_{12}\} - \frac{2V}{\hbar}\mathrm{Im}\ \rho_{12} \tag{8}$$

$$\frac{\partial \rho_{22}}{\partial t} = \hat{\mathscr{L}}_{22}\rho_{22} + \{V, \mathrm{Re}\ \rho_{12}\} + \frac{2V}{\hbar}\mathrm{Im}\ \rho_{12} \tag{9}$$

$$\frac{\partial \rho_{12}}{\partial t} = (\hat{\mathscr{L}}_0 - i\omega)\rho_{12} + \frac{1}{2}\{V, \rho_{12} + \rho_{22}\} + \frac{iV}{\hbar}(\rho_{11} - \rho_{22}) \tag{10}$$

where $\hat{\mathscr{L}}_\mu f = \{H_\mu, f\}$ defines the classical Liouville operator $\hat{\mathscr{L}}_\mu$ in terms of the Poisson bracket with the corresponding Hamiltonian. The average Hamiltonian $H_0 = (H_{11} + H_{22})/2$ appears in the equation of motion for the electronic coherence $\rho_{12}(\mathbf{q}, \mathbf{p}, t)$. In addition, an imaginary phase factor $-i\omega$ contributes a nonclassical component to the evolution of ρ_{12}, where $\omega = (H_{11} - H_{22})/\hbar$ is the difference potential divided by $\hbar$. The equation of motion for ρ_{21} can be obtained from eq 10 by complex conjugation. For nonzero electronic coupling V, sink and source terms appear in the equations that couple the evolving generalized phase space distributions to each other.

In the full numerical method, the functions ρ_{11}, ρ_{22}, and ρ_{12} are each represented by distinct ensembles of trajectories. Each trajectory is weighted by a time-dependent coefficient; for the coherence, these coefficients are, in general, complex numbers. In particular,

$$\rho_\mu(\Gamma, t) = \frac{1}{N}\sum_{j=1}^{N} a_j^{(\mu)}(t)\, \phi(\Gamma - \Gamma_j^{(\mu)}(t)) \tag{11}$$

where $\Gamma = (\mathbf{q}, \mathbf{p})$. Here, N is the number of trajectories in the ensemble (taken here to be the same for each μ), where $\mu = 11, 22, 12$. The trajectory ensembles are smoothed by a

Gaussian function $\phi(\Gamma)$:

$$\phi(\Gamma - \Gamma_o) = \prod_{n=1}^{f} \phi_n(\Gamma_n - \Gamma_{n,o}) \tag{12}$$

where

$$\phi_n(\Gamma_n - \Gamma_{n,o}) = \frac{1}{2\pi\sigma_{q,n}\sigma_{p,n}} \exp\left[-\frac{(q_n - q_{n,o})^2}{2\sigma_{q,n}{}^2} - \frac{(p_n - p_{n,o})^2}{2\sigma_{p,n}{}^2}\right] \tag{13}$$

The widths $\sigma_{q,n}$ and $\sigma_{p,n}$ are determined by numerical considerations. To use eq 11 as the basis for propagation of the coupled phase space functions, equations of motion for the coefficients $a_j^{(\mu)}(t)$ are needed. These are then combined with conventional Hamiltonian dynamics for the phase space variables $\Gamma_j^{(\mu)}(t) = (\mathbf{q}_j^{(\mu)}, \mathbf{p}_j^{(\mu)})$. In the full multiple ensemble implementation, each ensemble evolves under its own Hamiltonian H_μ.

We derive equations of motion for the trajectories and their coefficients by considering the short time limit of the integrated form of the inhomogeneous coupled linear partial differential equations given in eqs 8−10. As shown in our previous work,[1−5] the result is a set of linear algebraic equations relating the time t and $t + \Delta t$ coefficients:

$$\mathbf{a}^{(11)}(t + \Delta t) = \mathbf{a}^{(11)}(t) + \Delta t\left[[\mathbf{S}^{(11)}]^{-1}\mathbf{D}^{(10)}\mathbf{V}'(0)\ \mathrm{Re}\ \mathbf{a}^{(12)}(t) - \frac{2}{\hbar}[\mathbf{S}^{(11)}]^{-1}\mathbf{S}^{(10)}\mathbf{V}^{(0)}\ \mathrm{Im}\ \mathbf{a}^{(12)}(t)\right] \tag{14}$$

$$\mathbf{a}^{(22)}(t + \Delta t) = \mathbf{a}^{(22)}(t) + \Delta t\left[[\mathbf{S}^{(22)}]^{-1}\mathbf{D}^{(20)}\mathbf{V}'(0)\ \mathrm{Re}\ \mathbf{a}^{(12)}(t) + \frac{2}{\hbar}[\mathbf{S}^{(22)}]^{-1}\mathbf{S}^{(20)}\mathbf{V}^{(0)}\ \mathrm{Im}\ \mathbf{a}^{(12)}(t)\right] \tag{15}$$

$$\mathbf{a}^{(12)}(t + \Delta t) = \Phi^{(0)}\mathbf{a}^{(12)}(t) + \Delta t\left[\frac{1}{2}[\mathbf{S}^{(00)}]^{-1}\mathbf{D}^{(01)}\mathbf{V}'^{(1)} + \frac{1}{\hbar}[\mathbf{S}^{(00)}]^{-1}\mathbf{S}^{(01)}\mathbf{V}^{(1)}\right]\Phi^{(1)}\mathbf{a}^{(11)}(t) + \Delta t\left[\frac{1}{2}[\mathbf{S}^{(00)}]^{-1}\mathbf{D}^{(02)}\mathbf{V}'^{(2)} - \frac{1}{\hbar}[\mathbf{S}^{(00)}]^{-1}\mathbf{S}^{(02)}\mathbf{V}^{(2)}\right]\Phi^{(2)}\mathbf{a}^{(22)}(t) \tag{16}$$

(We employ the notation $\mu = 12 \equiv 0$ in these expressions for simplicity.) The overlap and derivative matrices $\mathbf{S}^{(\mu\nu)}$ and $\mathbf{D}^{(\mu\nu)}$ are defined at time t as follows:

$$S_{ij}^{(\mu\nu)} = \int\int \phi(\Gamma - \Gamma_i^{(\mu)})\phi(\Gamma - \Gamma_j^{(\nu)})\ \mathrm{d}^{2f}\Gamma \tag{17}$$

$$[D_{ij}^{(\mu\nu)}]_k = \int\int \phi(\Gamma - \Gamma_i^{(\mu)})\frac{\partial}{\partial p_k}\phi(\Gamma - \Gamma_j^{(\nu)})\ \mathrm{d}^{2f}\Gamma \tag{18}$$

These matrix elements can be evaluated analytically.[1−5] The diagonal matrices in eqs 14−16 are given by

$$\mathbf{V}_{ij}^{(\mu)} = V(\Gamma_i^{(\mu)})\delta_{ij} \tag{19}$$

$$[\mathbf{V}'^{(\mu)}_{ij}]_k = \frac{\partial V(\Gamma_i^{(\mu)})}{\partial q_k}\delta_{ij} \tag{20}$$

$$\Phi_{ij}^{(\mu)} = \mathrm{e}^{-\mathrm{i}\omega(\Gamma_i^{(\mu)})\Delta t}\delta_{ij} \tag{21}$$

During each time step, the coupled set of linear equations, eqs 14−16, are first solved for the updated coefficients and then the trajectories $\Gamma_j^{(\mu)}(t)$ are integrated forward to $t + \Delta t$ using Hamilton's equations.

The numerical method described above can give accurate results for model problems of molecular dynamics with electronic transitions.[2−5] The approach can describe both electronic relaxation processes and coherent wave packet interferometry with a nearly quantitative level of accuracy. In practice, however, the method requires care to apply to a given problem and is difficult to incorporate into a general "black box" approach that can be employed without significant preliminary study of the problem and its dynamics.

The origin of these complications is the use of multiple trajectory ensembles to support the elements of ρ. Each set of trajectories $\Gamma_j^{(\mu)}(t)$ must be followed in phase space. This is not a difficulty for the trajectory propagation itself, but it creates significant technical problems for the equations of motion describing the coefficients $a_j^{(\mu)}(t)$. In particular, the structure of the matrices $\mathbf{S}^{(\mu)}$ and $\mathbf{D}^{(\mu)}$ as a function of the trajectory indices i and j become complicated and unpredictable. Significant bookkeeping is thus required if approximations to the matrix structure are to be made to simplify and accelerate the linear algebraic computations. More seriously, divergence of the ensembles relative to one another in phase space can create situations where, e.g., the μth ensemble fails to provide an adequate representation of ρ_μ where the inhomogeneous term depending on $\rho_{\nu \neq \mu}$ is important because $\Gamma_j^{(\mu)}(t)$ and $\Gamma_j^{(\nu)}(t)$ no longer overlap in configuration and momentum space. Without significant effort being expended in generating new trajectories (and retiring irrelevant ones), the linear algebra problem for the coefficient evolution becomes ill-defined, resulting in numerical instabilities.

To circumvent the problem associated with a multiple trajectory ensemble representation of the density matrix elements, we have reformulated the semiclassical Liouville method in terms of a *single* reference ensemble $\Gamma_j^{(\mathrm{ref})}(t)$.[7] In particular, all three distribution functions are supported by a single trajectory ensemble, evolving under a reference Hamiltonian H_{ref}. For ultrafast relaxation of an initially excited electronic state (defined here as state 1), the dominant dynamical process is the evolution of the initial density ρ_{11}, and thus the natural choice for the reference Hamiltonian is $H_{\mathrm{ref}} = H_{11}$. The ensemble of trajectories supports the dynamics of ρ_{22} and ρ_{12}, as well as ρ_{11}. Incorporating a single reference ensemble in eq 11 gives the densities as

$$\rho_\mu(\Gamma, t) = \frac{1}{N}\sum_{j=1}^{N} a_j^{(\mu)}(t)\phi(\Gamma - \Gamma_j^{(\mathrm{ref})}(t)) \tag{22}$$

Propagating these different generalized distributions under the same Hamiltonian introduces errors in the evolution. To compensate for the error made in using the "wrong" trajectories in eq 22, a correction factor is incorporated into equations of motion for the coefficients $a_j^{(\mu)}(t)$. We write the propagators for the electronic states, $\exp(t\hat{\mathcal{L}}_\mu)$, in terms of the reference propagator $\exp(t\hat{\mathcal{L}}_{\mathrm{ref}})$. The μth Hamiltonian H_μ is expressed in terms of the reference Hamiltonians H_{ref} and a correction Hamiltonian ΔH_μ:

$$H_\mu = H_{\mathrm{ref}} + \Delta H_\mu \tag{23}$$

where $\Delta H_\mu = H_\mu - H_{\mathrm{ref}}$. Then, defining the Liouville operator $\hat{\mathcal{L}}_{\Delta H_\mu} \equiv \{\Delta H_\mu, \cdot\}$ and invoking a short time approximation, we have

$$\mathrm{e}^{\Delta t\hat{\mathcal{L}}_\mu} \simeq \mathrm{e}^{\Delta t\hat{\mathcal{L}}_{\mathrm{ref}}}\mathrm{e}^{\Delta t\hat{\mathcal{L}}_{\Delta H_\mu}} \simeq \mathrm{e}^{\Delta t\hat{\mathcal{L}}_{\mathrm{ref}}}(1 + \Delta t\hat{\mathcal{L}}_{\Delta H_\mu}) \tag{24}$$

The expressions for the short-time propagated ρ_μ then become

$$\rho_{11}(\Gamma, t+\Delta t) = e^{\Delta t \hat{\mathscr{L}}_{\rm ref}}[\rho_{11}(\Gamma, t) + (b_{11}(\Gamma, t) + \hat{\mathscr{L}}_{\Delta H_{11}}\rho_{11}(\Gamma, t))\Delta t + O(\Delta t^2)] \quad (25)$$

$$\rho_{22}(\Gamma, t+\Delta t) = e^{\Delta t \hat{\mathscr{L}}_{\rm ref}}[\rho_{22}(\Gamma, t) + (b_{22}(\Gamma, t) + \hat{\mathscr{L}}_{\Delta H_{22}}\rho_{22}(\Gamma, t))\Delta t + O(\Delta t^2)] \quad (26)$$

$$\rho_{12}(\Gamma, t+\Delta t) = e^{\Delta t \hat{\mathscr{L}}_{\rm ref}} e^{-i\omega(\Gamma)\Delta t}[\rho_{12}(\Gamma, t) + (b_{12}(\Gamma, t) + \hat{\mathscr{L}}_{\Delta H_0}\rho_{12}(\Gamma, t))\Delta t + O(\Delta t^2)] \quad (27)$$

A modified set of linear algebraic equations is obtained:[7]

$$\mathbf{a}^{(11)}(t+\Delta t) = (1 + \Delta t \mathbf{S}^{-1}\mathbf{D}\Delta_1')\mathbf{a}^{(11)}(t) + \Delta t\left[\mathbf{S}^{-1}\mathbf{D}\mathbf{V}' \,\mathrm{Re}\, \mathbf{a}^{(12)}(t) - \frac{2}{\hbar}\mathbf{V}\,\mathrm{Im}\,\mathbf{a}^{(12)}(t)\right] \quad (28)$$

$$\mathbf{a}^{(12)}(t+\Delta t) = (1 + \Delta t \mathbf{S}^{-1}\mathbf{D}\Delta_2')\mathbf{a}^{(22)}(t) + \Delta t\left[\mathbf{S}^{-1}\mathbf{D}\mathbf{V}' \,\mathrm{Re}\, \mathbf{a}^{(12)}(t) + \frac{2}{\hbar}\mathbf{V}\,\mathrm{Im}\,\mathbf{a}^{(12)}(t)\right] \quad (29)$$

$$\mathbf{a}^{(12)}(t+\Delta t) = (1 + \Delta t \mathbf{S}^{-1}\mathbf{D}\Delta_{12}')\Phi\mathbf{a}^{(12)}(t) + \frac{1}{2}\Delta t \mathbf{S}^{-1}\mathbf{D}\mathbf{V}'\Phi[\mathbf{a}^{(11)}(t) + \mathbf{a}^{(22)}(t)] + \frac{i}{\hbar}\Delta t \mathbf{V}\Phi[\mathbf{a}^{(11)}(t) - \mathbf{a}^{(22)}(t)] \quad (30)$$

The overlap, derivative, potential, potential derivative, and phase matrices now no longer are given superscripts indicating the ensemble, as for all cases $\mu = \nu \equiv$ ref.

As shown in ref 7, results obtained using the single ensemble Liouville formulation can be in close agreement with exact quantum results for model one-dimensional systems. Complications remain, however, for multidimensional problems: The number of trajectories required to represent the evolving densities accurately scale exponentially with the number of degrees of freedom *f*. Straightforward methods for solving the linear algebra problem associated with the interactions between trajectories quickly becomes computationally unfeasible, and additional approximations are required.

The main numerical complication of the interacting trajectory-based method is the linear algebra associated with the overlap matrix **S**. For the localized smoothing functions $\phi(\Gamma)$, this matrix is nonzero mainly along the diagonal. The other relevant object for coupling of trajectories is the derivative matrix **D**, which has zeros on the diagonal. These two characteristics suggest introducing the following *independent trajectory* approximation:

$$\mathbf{S}^{-1}\mathbf{D} = \mathbf{0} \quad (31)$$

With this approximation, the equations of motion for the coefficients simplify to

$$\mathbf{a}^{(11)}(t+\Delta t) = \mathbf{a}^{(11)}(t) - \frac{2\Delta t}{\hbar}\mathbf{V}\,\mathrm{Im}\,\mathbf{a}^{(12)}(t) \quad (32)$$

$$\mathbf{a}^{(22)}(t+\Delta t) = \mathbf{a}^{(22)}(t) + \frac{2\Delta t}{\hbar}\mathbf{V}\,\mathrm{Im}\,\mathbf{a}^{(12)}(t) \quad (33)$$

$$\mathbf{a}^{(12)}(t+\Delta t) = \Phi\mathbf{a}^{(12)}(t) + \frac{i\Delta t}{\hbar}\mathbf{V}\Phi[\mathbf{a}^{(11)}(t) - \mathbf{a}^{(22)}(t)] \quad (34)$$

Because now there are no cross terms, we can drop the matrix notation and write the iteration algorithm for the weights of each individual trajectory as

$$a_i^{(11)}(t+\Delta t) = a_i^{(11)}(t) - \frac{2\Delta t}{\hbar}V(\Gamma_i)\,\mathrm{Im}\, a_i^{(12)}(t) \quad (35)$$

$$a_i^{(22)}(t+\Delta t) = a_i^{(22)}(t) + \frac{2\Delta t}{\hbar}V(\Gamma_i)\,\mathrm{Im}\, a_i^{(12)}(t) \quad (36)$$

$$a_i^{(12)}(t+\Delta t) = e^{i\omega(\Gamma_i)\Delta t}\left(a_i^{(12)}(t) + \frac{i\Delta t}{\hbar}V(\Gamma_i)[a_i^{(11)}(t) - a_i^{(22)}(t)]\right) \quad (37)$$

where $i = 1, 2, ..., N$, and Γ_i is the phase space point of trajectory i at time t. This approximation forms the foundation of the method presented in this paper. It will be seen that for the problems for which this approximation works, the results show very good agreement when compared against exact calculations. Moreover, this formulation provides a significant advantage over coupled trajectory implementations of the semiclassical Liouville formulation of quantum dynamics: The computational cost required in the implementation of eqs 35, 36, and 37 is comparable to conventional classical molecular dynamics and ensemble averaging.

In the next section the independent trajectory approach will be tested on the model problems considered in our previous work to compare its accuracy and asses its limitations. The method is then extended to the reaction dynamics in a two-dimensional model of collinear reaction dynamics.

III. Numerical Tests of Method

A. Coupled Bound−Repulsive System. As a first test of the accuracy of the single ensemble independent trajectory approach, we apply the method to a model of coupled bound and repulsive motion on a pair of one-dimensional potentials. This system was treated in our previous publications using the full multiple ensemble method[2−4,18] and the single ensemble implemention.[7] Nearly quantitative agreement with quantum wave packet results was obtained in both of these previous studies.

The system represents the coupled electronic-nuclear dynamics of a diatomic molecule with (reduced) mass $m = 10\,000$ au prepared initially as a minimum uncertainty wave packet on the upper (repulsive) surface. The initially populated state is represented by an exponential function,

$$U_1(q) = Ae^{-\alpha}(q - q_1) - B \quad (38)$$

which is coupled by off-diagonal terms in the diabatic two-state Hamiltonian to a bound Morse potential, given by

$$U_2(q) = D(e^{-2\beta(q-q_2)} - 2e^{-\beta(q-q_2)}) \quad (39)$$

These curves exhibit a single crossing in the dynamically relevant region, at $q = q_c$. The off-diagonal coupling term is represented by a Gaussian centered at the crossing point,

$$V(q) = V_0 e^{-c(q-q_c)^2} \quad (40)$$

Numerical values of the parameters for this system are given in Table 1.

The initially populated repulsive state is employed to define the reference Hamiltonian $H_{\rm ref}$, and so trajectories are propagated on the $U_1(q)$ potential. An initial ensemble of $N = 169$ trajectories is generated in phase space by sampling the two-dimensional Gaussian Wigner distribution of the initial mini-

TABLE 1: Numerical Values of Parameters for the Bound−Repulsive System, in Atomic Units

A	2.2782×10^{-2}
B	2.2782×10^{-2}
α	2.0
q_1	5.5
D	1.8225×10^{-2}
β	1.0
q_2	5.8
c	4.0
q_c	6.15315
m	1×10^4
ω	4×10^{-3}
V_0	1.2×10^{-3}

mum uncertainty wave packet localized at (q_o, $p_o = 0$) on the upper surface. This initial wave packet is parametrized by the harmonic frequency ω given in Table 1, giving widths $\Delta_q = \sqrt{\hbar/2m\omega}$ and $\Delta_p = \sqrt{m\omega\hbar/2}$, so that $\Delta_q\Delta_p = \hbar/2$. The repulsive wall of the potential accelerates the quantum state (and the trajectories in its ensemble representation) in the direction of increasing q, leading to electronic population transfer near the crossing point $q = q_c$.

The width parameters characterizing the smoothing function $\phi(q, p)$ are obtained from the initial wave packet widths by the scaling $\sigma_q = 2\Delta_q/N$ and $\sigma_p = 2\Delta_p/N$. These values are found to yield numerically stable and accurate results in practice. The exact quantum results were obtained by the method of Kosloff.[27]

As shown in Figure 1, the independent trajectory results are very close to the coupled single trajectory results of ref 7. For small initial displacements q_o, the initial wave packet has a relatively high kinetic energy at the crossing point. For such conditions, the semiclassical results agree very well with exact quantum calculations. Only when the initial wave packet is situated near the crossing point initially do the results disagree. These results indicate that the independent trajectory approximation does not introduce errors beyond those of the semiclassical method and its single ensemble formulation for this system.

B. Tully's Single Crossing Model. As a further test of the independent ensemble method, we consider a model proposed by Tully.[28] This model, which consists of two potentials with a single crossing, has become a benchmark problem for nonadiabatic dynamical simulation methods. We define the two diabatic surfaces to be

$$U_1(q) = \begin{cases} A[1 - \exp(Bq)] & q < 0 \\ -A[1 - \exp(-Bq)] & q > 0 \end{cases} \quad (41)$$

and

$$U_2(q) = -U_1(q) \quad (42)$$

The off-diagonal coupling is given by

$$V(q) = C \exp(-Dq^2) \quad (43)$$

These potentials exhibit a crossing at $q = 0$. Surface 1 defines H_{ref}. The numerical parameters employed are $A = 0.01$, $B = 1.6$, $C = 0.005$, and $D = 1.0$. The mass is $m = 2000$ au. We compute the final energy-dependent electronic transition probabilities P_1 and P_2, defined as the asymptotic populations of states 1 and 2, respectively. We show the results in Figure 2 and consider a range of initial average energies, given by $E = \hbar^2k^2/2m$, where k is the wave vector of the initial wave packet. The initial coordinate value chosen is $q_o = -6.0$ au, well to the left of the crossing point at $q = 0$, and the mean momentum is $p_o = \hbar k$. The position and momentum widths are chosen in the same manner as for the bound−repulsive system described above. The wave packet's initial Wigner function is again sampled with $N = 169$ trajectories. The exact results are obtained using by solving the time-dependent Schrödinger equation using the method of Kosloff.[27]

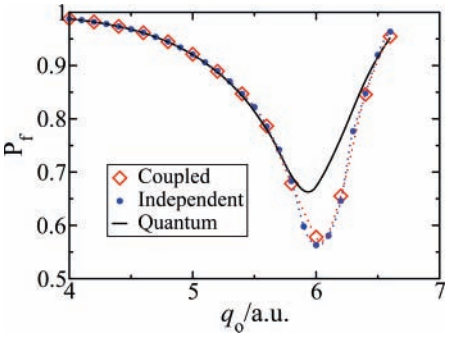

Figure 1. Exact and semiclassical asymptotic population on the repulsive surface as a function of the initial wave packet position for the coupled bound−repulsive model. Shown are wave packet propagation calculations (black), coupled trajectory results (red diamonds), and the calculations performed with the independent trajectory method (blue dots).

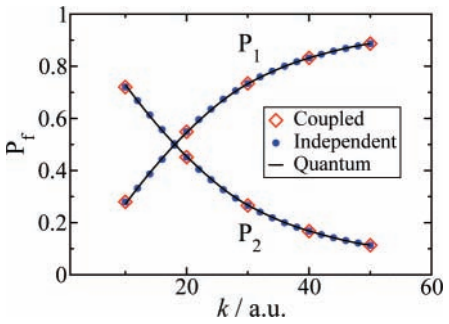

Figure 2. Final population for the single crossing model. The asymptotic population is studied for different initial momenta of the wave packet. Shown are wave packet propagation calculations (black), coupled trajectory results (red diamonds), and the calculations performed with the independent trajectory method (blue dots).

The results presented in Figure 2 show nearly quantitative agreement between the quantum and semiclassical Liouville results. The independent trajectory method gives results that are esentially indistinguishable from the interacting ensemble approach.

C. Tully's Dual Crossing Model. We also consider the dual crossing model of Tully.[28] This system exhibits two crossings, which allows for interference effects in the final state populations due to crossing and recrossing between the surfaces. The two potentials characterizing the dual crossing model are given by

$$U_1(q) = -A \exp(-Bq^2) + E_0 \quad (44)$$

and

$$U_2(q) = 0 \quad (45)$$

and the electronic coupling is taken to be

$$V(q) = C \exp(-Dq^2) \quad (46)$$

The numerical parameters are $A = 0.1$, $B = 0.28$, $E_0 = 0.05$, $C = 0.015$, $D = 0.06$, and $m = 2000$ au, the same as considered by Tully[28] and in our previous work on the single ensemble approach.[7] The reference Hamiltonian H_{ref} is defined by the $U_1(q)$ potential. The minimum uncertainty wave packet width is

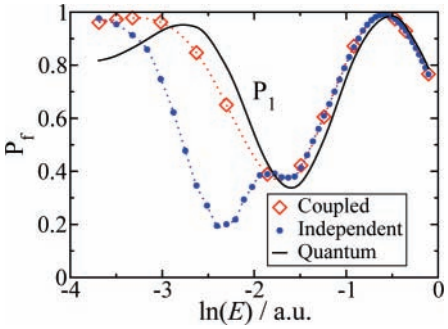

Figure 3. Final population for the dual crossing model. In this figure the asymptotic population is plotted against the logarithm of the initial kinetic energy of the wave packet. Shown are wave packet propagation results (black), coupled trajectory (red diamonds), and the calculations performed with the independent trajectory method (blue dots).

TABLE 2: Parameters Used in the Collinear Nonreactive Triatomic Reaction (All Values in Atomic Units)

D_e	β	r_e	D_{rep}	V_c	m
0.038647	0.458038	5.0494	0.02	0.00136	12652.7

the same as for the calculations described above, and the mean position and momentum are $q_o = -8.0$ au and $p_o = \hbar k$, where $E = \hbar^2k^2/2m$. The results are shown in Figure 3. Very good agreement is observed at high energies. However, strong deviations between the independent and coupled trajectory methods are seen at lower energies, and here the agreement between the independent trajectory results and exact quantum calculations is worse than those for the coupled trajectory approach. At the low energies, quantum effects are more important, and the nonlocal interference between amplitudes on the two electronic surfaces are not well-captured by the approximations underlying the current method.

D. Multidimensional Models. We now extend the independent trajectory formulation to the study a problem that has more than one spatial dimension. The model is two-dimensional and represents a collinear collision and reaction between an atom and a diatomic molecule, of the form A + BC → AB + C. We treat a system employed by Ben-Nun and Martínez in the study of their multiple spawning method for multidimensional nonadiabatic problems,[29] where values for the reaction probability have been given for quantum calculations and for simulations done with the multiple spawning method. In this two-dimensional diabatic model, each of the two diabatic potentials describes a collinear nonreactive collision between an atom and a diatomic molecule. Chemical reaction corresponds to transition between these two diabatic states. The interstate coupling has been set to a constant throughout the simulation. The calculations are done in Jacobi coordinates,[30] giving a diagonal kinetic energy operator for each electronic state. The two potential surfaces are given by

$$U_1(r, R) = D_e(1 - \exp(-\beta(r - r_e)))^2 + D_{rep}\exp(-\beta(R - r/2 - r_e)) \quad (47)$$

and

$$U_2(r, R) = D_e(1 - \exp(-\beta(R - r/2 - r_e)))^2 + D_{rep}\exp(-\beta(r - r_e)) \quad (48)$$

The Jacobi coordinate r represents the distance between atoms BC, and R is the distance from atom A to the center of mass of BC. As mentioned above, the kinetic energy operator is diagonal in this representation and is given by

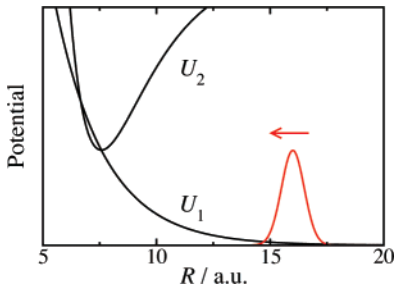

Figure 4. Potential energy landscape for the triatomic reaction model. The cut in the two-dimensional surface has been made at $r = r_e$.

$$T = \frac{p_r^2}{2M_{BC}} + \frac{p_R^2}{2M_{A,BC}} \quad (49)$$

and the intersurface coupling is

$$V = V_c \quad (50)$$

and the parameters M_{BC} and $M_{A,BC}$ are the reduced masses for the B−C and A−BC motions. The three atoms are taken to be identical with a mass of lithium, so the expressions for the reduced masses simplify to

$$M_{BC} = m/2 \quad \text{and} \quad M_{A,BC} = 2m/3 \quad (51)$$

The values of the different parameters used in the simulation are summarized in Table 2, where all the quantities are in in atomic units. A cut of the two-dimensional diabatic potential landscape is shown in Figure 4. This cut was made at $r = r_e$, which is taken as the center of the initial wave packet along the r coordinate, whereas the initial state center along R is taken at an asymptotic value with $R = 16$ au. The initial population is on surface 1; therefore, to get to the reactive region, some initial kinetic energy has to be given to the wave packet at the beginning of the simulation. The adiabatic representation of this two-dimensional system has two potential wells on the ground state, which describes a reactive atom exchange reaction of the LEPS form,[30] with an energy barrier separating the wells. The adiabatic representation is obtained from the diagonalization of the Hamiltonian for the system, and the barrier height is found to be $B_h = 0.43536$ eV.[29] Because this is the energy needed to overcome the barrier in the adiabatic representation, it will be the energetic reference in the measure of the initial kinetic energy of the wave packet:

$$T_{ex} = T - B_h \quad (52)$$

where the excess kinetic energy is calculated from the initial relative kinetic energy of the atom with respect to the center of mass of the diatomic molecule.

The semiclassical Liouville reaction probability is plotted against the excess kinetic energy in Figure 5 and compared with the results of exact quantum calculations.[29] Our semiclassical results show a very good correspondence with quantum calculations, with the best agreement at low and high energies.

IV. Summary

In this paper, we have presented an independent trajectory implementation of semiclassical Liouville method for simulating quantum processes using classical trajectories. The method is based on employing one ensemble of trajectories to represent

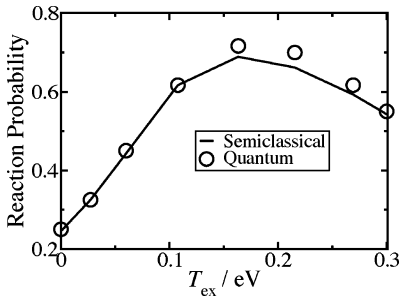

Figure 5. Reaction probability as a function of the excess kinetic energy. The curve labeled semiclassical refers to independent trajectory Liouville results. Quantum results are taken from ref 29.

all semiclassical density matrix elements of a coupled electronic state problem. The ensemble evolves classically under a single reference Hamiltonian, which is chosen on the basis of physical grounds. In the present work, an additional uncoupled trajectory approximation was introduced, allowing the members of the ensemble to evolve independently of one another. This independent trajectory approximation leads to great simplification in the implementation, while giving results of accuracy comparable to the semiclassical method itself for many problems. When the nonlocality of quantum dynamics becomes important, however, the deficiencies of the "more classical" independent ensemble approach become visible. The accuracy of the method was assessed for several model one-dimensional problems. An application to the chemical reaction dynamics of a collinear triatomic system was then presented, yielding excellent agreement with exact calculations. This method allows molecular dynamics involving coupled electronic surfaces to be modeled with essentially the same effort as classical molecular dynamics and ensemble averaging.

Acknowledgment. This work was supported by the National Science Foundation.

References and Notes

(1) Martens, C. C.; Fang, J. Y. *J. Chem. Phys.* **1997**, *106*, 4918−4930.
(2) Donoso, A.; Martens, C. C. *J. Phys. Chem. A* **1998**, *102*, 4291−4300.
(3) Donoso, A.; Martens, C. C. *J. Chem. Phys.* **2000**, *112*, 3980−3989.
(4) Donoso, A.; Kohen, D.; Martens, C. C. *J. Chem. Phys.* **2000**, *112*, 7345−7354.
(5) Donoso, A.; Martens, C. C. *Int. J. Quantum Chem.* **2002**, *90*, 1348−1360.
(6) Riga, J. M.; Martens, C. C. *J. Chem. Phys.* **2004**, *120*, 6863−6873.
(7) Roman, E.; Martens, C. C. *J. Chem. Phys.* **2004**, *121*, 11572.
(8) Kapral, R.; Ciccotti, G. *J. Chem. Phys.* **1999**, *110*, 8919.
(9) Kapral, R. *J. Phys. Chem. A* **2001**, *105*, 2885.
(10) Nielsen, S.; Kapral, R.; Ciccotti, G. *J. Chem. Phys.* **2000**, *112*, 6543.
(11) Kernan, D. M.; Ciccotti, G.; Kapral, R. *J. Chem. Phys.* **2002**, *116*, 2346.
(12) Wan, C. C.; Schofield, J. *J. Chem. Phys.* **2000**, *112*, 4447.
(13) Wan, C. C.; Schofield, J. *J. Chem. Phys.* **2000**, *113*, 7047.
(14) Wan, C. C.; Schofield, J. *J. Chem. Phys.* **2002**, *116*, 494.
(15) Ando, K. *Chem. Phys. Lett* **2002**, *360*, 240−242.
(16) Ando, K.; Santer, M. *J. Chem. Phys.* **2003**, *118*, 10399−10406.
(17) Santer, M.; Manthe, U.; Stock, G. *J. Chem. Phys.* **2001**, *114*, 2001−2012.
(18) Donoso, A.; Martens, C. C. *J. Chem. Phys.* **2002**, *116*, 10598.
(19) Lam, K. S.; George, T. F. In *Semiclassical Methods in Molecular Scattering and Spectroscopy*; Child, M. S., Ed.; Reidel: Dordrecht, The Netherlands, 1980.
(20) Cohen-Tannoudji, C.; Diu, B.; Laloe, F. *Quantum Mechanics*; Wiley: New York, 1977.
(21) Schatz, G. C.; Ratner, M. A. *Quantum Mechanics in Chemistry*; Prentice Hall: Englewood Cliffs, NJ, 1993.
(22) Wigner, E. P. *Phys. Rev.* **1932**, *40*, 749−759.
(23) Takahashi, K. *Prog. Theor. Phys. Suppl.* **1989**, *98*, 109−156.
(24) Lee, H. W. *Phys. Rep.* **1995**, *259*, 147−211.
(25) Mukamel, S. *Principles of Nonlinear Optical Spectroscopy*; Oxford University Press: Oxford, U.K., 1995.
(26) Goldstein, H. *Classical Mechanics*, 2nd ed; Addison-Wesley: Reading, MA, 1980.
(27) Kosloff, R. *Annu. Rev. Phys. Chem.* **1994**, *45*, 145.
(28) Tully, J. C. *J. Chem. Phys.* **1990**, *93*, 1061.
(29) Ben-Nun, M.; Martinez, T. J. *J. Chem. Phys.* **1998**, *108* (17), 7244−57.
(30) Levine, R. D.; Bernstein, R. B. *Molecular Reactions Dynamics and Chemical Reactivity*; Oxford University Press: Oxford, U.KI., 1987.